DOI: 10.1002/ejic.201100651

Thermal Stability of $(K_xNa_yH_{1-x-y})_2Ti_6O_{13}$ Nanofibers

Michael B. Cortie,*[a] Linda Xiao,[a] Laszlo Erdei,[b][‡] Catherine S. Kealley,[a] Annette R. Dowd,[a] Justin A. Kimpton,[c] and Andrew M. McDonagh[a]

Keywords: Nanostructures / Nanofibres / Layered compounds / High-temperature chemistry / Titanates / Solid-state reactions

Potassium-rich titanate nanofibers were produced by digesting TiO_2 in concentrated KOH solutions under hydrothermal conditions. The nanofibers were characterized by scanning electron microscopy, energy dispersive X-ray spectroscopy, X-ray diffraction, and thermogravimetric analysis. A hexatitanate structure was assigned, in contrast to the trititanate structure usually resulting from NaOH treatment of TiO_2. The potassium cations could be exchanged with others, such as sodium, hydrogen, and ammonium. The potassium-rich hexatitanate was found to be photocatalytic in its as-synthesized condition. The thermal stability of the fibers during calcination was followed in situ using X-ray diffraction and was found to be strongly dependent on the chemical composition. The potassium-rich titanate converted to anatase at only 480 °C, whereas the hydrogen- and ammonium-rich materials had to be heated to over 600 °C before conversion took place. Conversion was notably slowest in the ammonium-rich material. Surprisingly, the sodium-rich hexatitanate did not form anatase at temperatures up to 800 °C and instead recrystallized.

Introduction

Nanofibers comprising titanate or titanium dioxide are of considerable interest because of their broad range of potential technological applications,[1] for example in photocatalysis,[2–5] as Li^+ reservoirs in lithium ion cells,[6] and as absorbents to sequester toxic metal ions[7,8] and radionucleides.[9] In photocatalysts, electron-hole pairs (excitons) are created in the material by light. Any holes that diffuse to the surface of the catalyst particle can act as a strong oxidant, whereas any electrons that reach the surface will act as a reductant. Nanoparticulate anatase has been intensively investigated in this regard[10] since the discovery[11] of its photocatalytic efficacy in 1971. Although most current titania-based photocatalysts are based on spherical nanoparticles, the use of a fibrous material, woven into a porous mat, may offer some technological advantages for absorption or oxidation of impurities.[12] In particular, although suspended (slurry) type reactors are popular due to their simplicity and high efficiency,[13] there is a need to separate the fine catalyst particles from the treated water afterwards.[3] Although the use of inert membranes to retain the photocatalyst particles can resolve this problem[14] (at increased complexity and cost), a better solution could to be apply the catalyst itself as a porous, textile-like filter.

In principle, filters of this type have become possible since the discovery of processes to make titania or titanate nanotubes and fibers by hydrothermal treatment.[15,16] However the formation, structure, morphology, and properties of these and other fibrous titanates are not yet completely understood.[1,17–19] Most investigations have been conducted on fibers grown in NaOH solution[2–4,7,8,16,19–23] but even in this relatively well-studied system there is still disagreement about the composition and structure of the fibers, and the mechanisms of their formation and/or destruction. Here, however, we report an investigation on the nanofibers produced by hydrothermal digestion of TiO_2 in concentrated KOH solution. There have been few studies of this system, possibly because of the lower yield and the need to use higher temperatures and pressures than reactions in NaOH.[24] In the literature, the identity of the product(s) formed by hydrothermal digestion of TiO_2 using KOH is vexed. There are many polymorphs of the type $K_2Ti_nO_{2n+1}$, such as layer (n = 2 and 4) and tunnel (n = 6 and 8)[5] structures, and many of these can have the K^+ partially ion-exchanged with H^+ and/or contain water of hydration. Fully protonated titanates belong to a large family with the generic formula $H_{2m}Ti_nO_{2n+m}$.[1] At least five different phases of titanate in fibers produced by hydrothermal treatment of TiO_2 powder in concentrated KOH have been reported. Some relevant data is summarized in Table 1. A

[a] Institute for Nanoscale Technology, University of Technology Sydney,
P. O. Box 123, Broadway, NSW 2007, Australia
E-mail: michael.cortie@uts.edu.au
[b] Institute for Water and Environmental Resources Management, University of Technology Sydney,
P. O. Box 123, Broadway, NSW 2007, Australia
[c] Australian Synchrotron,
800 Blackburn Road, Clayton, VIC 3168, Australia
[‡] Current address: Faculty of Engineering and Surveying, University of Southern Queensland,
West Street, Toowoomba, QLD 4350, Australia
Supporting information for this article is available on the WWW under http://dx.doi.org/10.1002/ejic.201100651.

Table 1. Identity assigned to fibers produced by hydrothermal treatment of Degussa P25, anatase, rutile or amorphous TiO_2 in concentrated KOH. The published patterns that are similar in terms of peak position and shape to those found in this work are indicated.

Source	Similar XRD pattern to this work	Reactant	Temp. [°C]	Time [d]	Phase(s) reported
Boyle[25]	yes	10 M KOH	120–185	3–7	$H_2Ti_2O_5{\cdot}H_2O$ or TiO_2-B
Amano[5]	yes	17 M KOH	110	1	$K_{0.74}H_{1.26}Ti_4O_9$
Daoud[17]	no	10 M KOH	80–110	3	TiO_2-B
Meng[26]	yes	15 M KOH	180	4	$K_2Ti_6O_{13}$
Nakahira[27]	no	10 M KOH	110	2	$H_2Ti_4O_9{\cdot}H_2O$
Yuan[28]	yes	8 M KOH	200	2	$K_2Ti_8O_{17}$
Du[29]	yes	10 M KOH	130	3	$K_2Ti_6O_{13}$

range of source materials were used in the work listed and, in general, seed particle size and phase were found to affect the kinetics of the reaction and the morphology, but not the identity, of the product. Furthermore, the thermal stability of these materials is not yet well characterized. Here we consider the structure and properties of these fibers, both in the as-synthesized form, and after partial ion-exchange of the K^+ with H^+, Na^+ or NH_4^+. The phenomena accompanying their calcination are examined in detail. Significant differences in the thermal stability and behavior of the various compounds were found.

Results

As-Produced Fibers

Scanning electron microscopy (SEM) images of the various fibers after hydrothermal treatment, washing, ion-exchange, and drying are shown in Figure 1. The initial potassium-rich titanate (Figure 1, a) consists of nanofibers of 5–50 nm diameter (measured using SEM) with lengths in excess of 1 μm. These dimensions are similar to those reported by Amano et al.[5] who also reacted TiO_2 with KOH. After ion-exchange, the H^+-, Na^+-, and NH_4^+-substituted titanates maintained the fibrous morphology (Figure 1, b–d). The images also suggest that the fibers are not of circular cross-section but may be ribbon-like, the so-called nanobelt morphology.

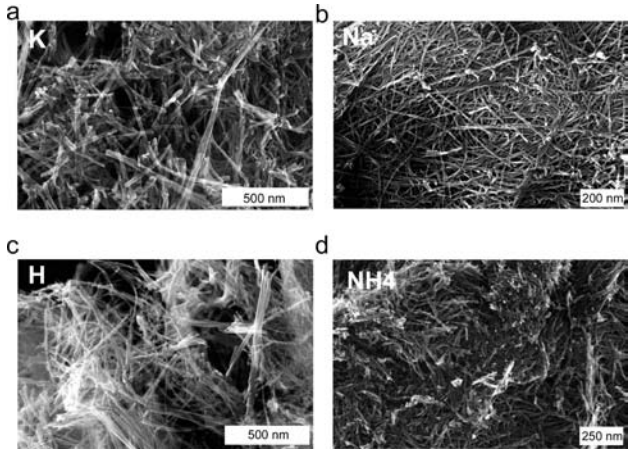

Figure 1. SEM images of the sinuous titanate nanofibers produced by hydrothermal processing: (a) potassium-, (b) sodium-, (c) hydrogen-, and (d) ammonium-rich titanate.

X-ray diffraction patterns of the fibers are shown in Figure 2. The patterns of the samples are all very similar, which indicates that the basic crystal structure of the compound did not change much during the ion-exchange process. The peaks are, however, relatively broad due to the nanocrystalline structure of the fibers and, possibly, the presence of lattice defects. Comparison to the standard patterns from the Joint Committee on Powder Diffraction Standards (JCPDS) Crystallography Open Database (http://www.crystallography.net/) and the literature indicated that $K_2Ti_6O_{13}$ was the best match to the present product, even though the usually strong (–2 0 1) peak at 13.8° (the 2θ position for Cu-K_α radiation) is absent. The diffraction data collected in this work does not correlate to any of the standard patterns for the other compounds listed in Table 1. Patterns that are very similar to these were published by Boyle et al.[25] for fibers made by a process similar to that used here but in their case were tentatively assigned to either the $H_2Ti_2O_5{\cdot}H_2O$ or TiO_2-B phases. The structures of titanate fibers produced by the various routes are considered again in greater detail in the Discussion.

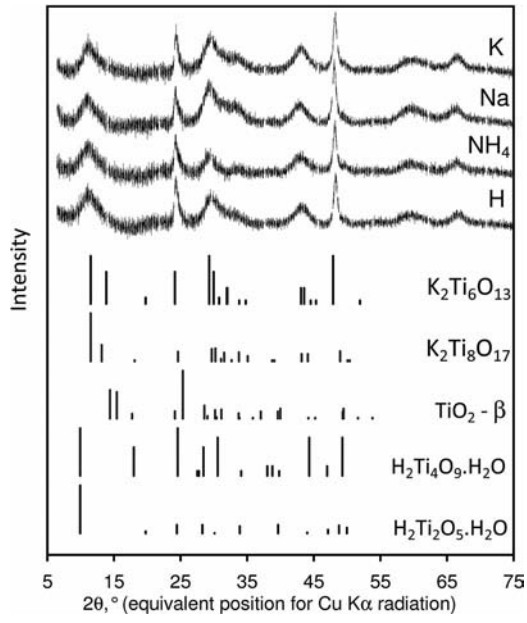

Figure 2. X-ray diffraction patterns of the washed and dried fibers. The peaks for well crystallized $K_2Ti_6O_{13}$ (JCPDS card 00-040-0403), $K_2Ti_8O_{17}$ (00-041-1100), TiO_2-β (00-046-1238), $H_2Ti_4O_9{\cdot}H_2O$ (00-036-0655), and $H_2Ti_2O_5{\cdot}H_2O$ (00-047-0124) are also shown. The experimental patterns are best matched by the standard pattern for the hexatitanate.

Characterization of Potassium-Rich Titanate Fibers

Preparation of a sample of potassium-rich titanate for TEM analysis by sonication in water for 30 min caused the fibers to break into segments of ca. 10 nm wide by up to 100 nm long (an occurrence also noted by others).[19,30] Although the width of the segments matches the width of the fibers observed in the SEM images, the length is obviously very much shorter. The segments were not hollow (Figure 3, a and b) and a characteristic layered structure was clearly visible (Figure 3, c).[17] This is unlike the case for the fibers produced using NaOH, which are often (but not invariably) reported as hollow.[4,7,20,23] The interlayer spacing observed in the TEM images was approximately 0.75 ± 0.03 nm. Interplanar spacings of between 0.75 and 0.88 nm have been reported for other layered titanates.[5,23,31] These layers, which correspond to the (2 0 0) planes of the unit cell, generate an XRD peak in the vicinity of $2\theta = 11°$ when Cu-K_α radiation is used. The presence of this peak is evidence that one of the layered or tunnel titania structures has formed,[4,5,31] and the converse may be deduced from its absence in randomly oriented powder samples. The electron diffraction pattern of the washed and sonicated sample (Table 2 and inset c in Figure 3), however, was more similar to that of TiO_2-B than $K_2Ti_6O_{13}$. We suggest that the protracted washing and sonication in water may have resulted in the extraction of K^+ from $K_2Ti_6O_{13}$ and its conversion to short pieces of pseudomorphous layered TiO_2-B, a process already known to occur in other types of titanate fibers.[2,17,32]

The fit of the putative $K_2Ti_6O_{13}$ structure to the X-ray diffraction pattern of the K-rich material was explored further by simulating the patterns with a degree of disorder (Figure 3, d). A pattern calculated from a CIF file for $K_2Ti_6O_{13}$, but with all peaks broadened by imposing a Gaussian shape with a width of 1.5°, is shown as *ii*. This pattern is similar to the experimental data except that the sharp peaks for the (1 1 0) and (0 2 0) planes in the measured pattern are less intense and broader in the simulated pattern. Although anatase also has peaks at these positions, the peaks seen here cannot be from anatase because its other characteristic peaks are absent. The peak corresponding to the interplanar spacing of ca. 0.75 nm observed by TEM is matched by a peak at a 2θ position of 11.5° in the 2θ scale corresponding to Cu-K_α radiation (corresponding to a lattice spacing of about 0.77 nm). Finally, the different shape of the (1 1 0) and (0 2 0) peaks was investigated further by constructing an ensemble average of 55 calculated powder diffraction patterns (each with a Gaussian broadening of 0.72° on the peaks) with the *c* parameter of the unit cells drawn from a Gaussian distribution centered on 1.65 nm and a standard deviation of 0.17 nm. The *b* parameter of these lattice cells was adjusted to 0.3778 nm so that the position of the (0 2 0) peak was correctly matched. This pattern, designated as *iii*, is quite similar to the experimental data, although the disorder and nanocrystallinity in the experimental material may be responsible for the broadening and merging of the (2 0 1) and (2 0 –1) peaks.

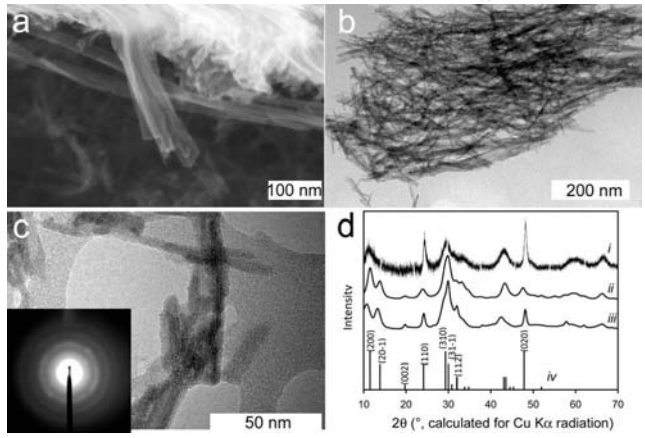

Figure 3. (a) High magnification SEM image of the tip of a bundle of potassium-rich fibers showing that they are not hollow. (b) TEM image of a patch of potassium-rich fibers. (c) High-magnification TEM image of a potassium-rich fiber showing its layered structure. The electron diffraction pattern inset is similar to that of anatase. (d) X-ray diffraction patterns for as-synthesized and washed potassium-rich fibers, showing *i*) measured data, *ii*) pattern calculated from a cif file for $K_2Ti_6O_{13}$ using a 1.5° Gaussian spread of the peaks, *iii*) a pattern obtained as an ensemble average of 55 structures with a Gaussian spread of interlayer spacings (see text), and *iv*) a stick plot from JCPDS card 00–040–0402.

Chemical Composition

Energy dispersive X-ray spectroscopy (EDS) analysis in the SEM indicated that the K/Ti ratio in the as-synthesized (and washed) potassium-rich fibers was 0.168 ± 0.005. If the formula of the acid-washed material is accepted as $(K_xH_{1-x})_2Ti_6O_{13}$, then a mean stoichiometry of $(K_{0.5}H_{0.5})_2Ti_6O_{13}$ and a range between $(K_{0.49}H_{0.51})_2Ti_6O_{13}$ and $(K_{0.52}H_{0.48})_2Ti_6O_{13}$ is inferred. Acid treatment of the $(K_{0.5}H_{0.5})_2Ti_6O_{13}$ potassium-rich titanate fibers to produce hydrogen-rich titanate lowered the K content further to a mean stoichiometry of $(K_{0.3}H_{0.7})_2Ti_6O_{13}$ as determined by SEM EDS analysis of the heavier elements. After ion ex-

Table 2. Analysis of the strongest electron diffraction rings of the washed and sonicated TEM sample of potassium-rich titanate (*d*: lattice spacing).

Measured *d* [nm]	Equivalent Cu-K_α 2θ	cf. TiO_2-B *d* [nm]	TiO_2-B plane
0.25 +0.01, –0.02	36° +/–2°	0.269, 0.270	(3 1 0), (–3 1 1)
0.19 +/–0.01	48° +3°, –2°	0.203, 0.208	(0 0 3), (–6 0 1)
0.175 +/–0.01	52° +/–3°	0.173	(1 1 3)

change in NaOH and washing, the sodium-rich fibers had a mean Na/K ratio of ca. 2.15, and a (Na + K)/Ti ratio of ca. 0.35, which gives a composition in the vicinity of $(K_{0.30}Na_{0.70})_2Ti_6O_{13}$ to $(K_{0.35}Na_{0.65})_2Ti_6O_{13}$. Importantly, in this treatment the Na^+ has displaced the H^+ but not affected the K^+ content. This sample also contained about 1 at.-% Si (expressed as an atomic fraction that excludes hydrogen), which indicates that the NaOH had extracted silicon ions from the surface of the glassware.

The portion of the hydrogen-rich titanate that had been immersed in NH_4OH solution had a nominal stoichiometry of $(K_{0.26}Na_{0.11}X_{0.63})_2Ti_6O_{13}$, where X is assigned as NH_4^+. Once again, the K content was not significantly altered. However, the sample also contained up to 3 at.-% Si and Na (expressed as an atomic fraction that excludes hydrogen). It is possible that the sample contained a small proportion of a Si-containing phase such as $HK_3Ti_4O_4(SiO_4)_3{\cdot}4H_2O$ (cf. Boyle et al.[25]) but no evidence for this was found in the XRD patterns.

Thermal Stability

Figure 4 shows SEM and TEM images of the potassium-rich titanate product after calcination at 450 and 700 °C. Upon calcination at 700 °C, the fibers crystallized into smaller rods of between 20 and 30 nm in diameter and up to 100 nm in length, however, the layered structure of a titanate is still clearly visible in the TEM image. The material changes from fibrous to rod-like between 450 and 700 °C. In situ XRD experiments, Figure 5, revealed that anatase crystallized from the fibers starting at 480 °C. By 600 °C the sample was mostly anatase with only a small proportion of the hexatitanate phase remaining (Figure 5, b). However, a broad peak at $d = 0.75 \pm 0.01$ nm (2θ of 11.8° when scaled to Cu-K_α radiation) shows that some layering of the structure still persisted at 600 °C, in agreement with the TEM image in Figure 4. The relative proportions of the phases present were followed by calculating the areas of the (1 1 0) peak of the titanate and the (1 0 1) peak of the anatase (Figure 5, c). Because these two peaks lie quite close together, it was necessary to fit them simultaneously using two pseudo-Voight functions and a linear trend for the background. The stability of the fit was enhanced by setting the shape parameter of each peak to 1.0, the HWHM parameter of the titanate

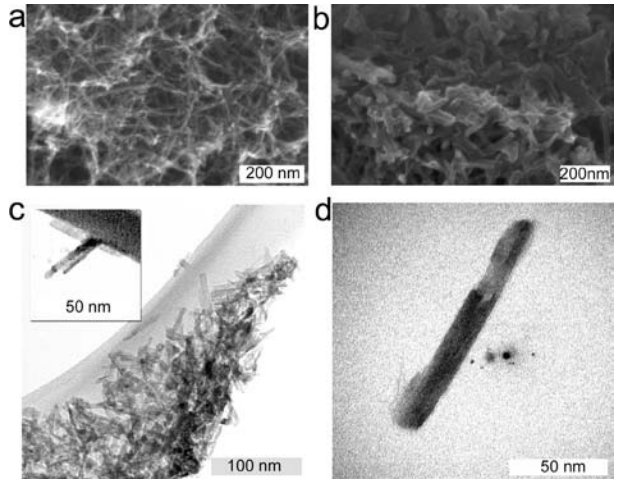

Figure 4. Microstructure of the nanofibers and nanorods produced by calcination of the potassium titanate. SEM micrographs at (a) 450 °C and (b) 700 °C and TEM micrographs at (c) 450 °C and (d) 700 °C. The (2 0 0) planes are still clearly visible in the TEM images, even in the sample calcined at 700 °C.

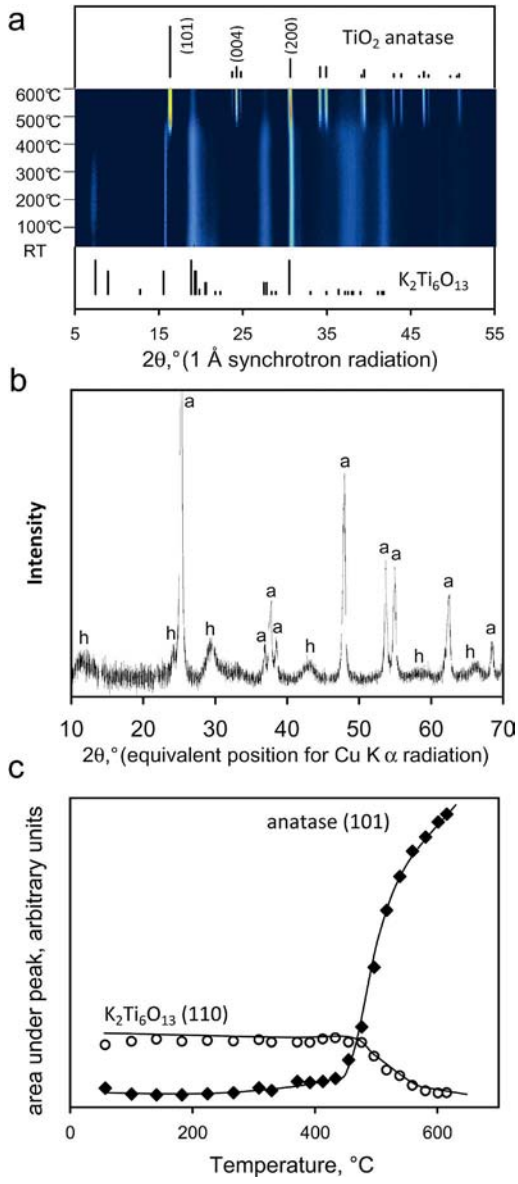

Figure 5. (a) X-ray diffraction map of the potassium-rich sample as a function of temperature. There is no anatase in the sample at room temperature. The (1 0 1) peak of anatase becomes visible at 480 °C. At 620 °C the sample is substantially composed of anatase. JCPDS entries for anatase (card 00-021-1272) and $K_2Ti_6O_{13}$ (card 00-040-0403) are shown as stick plots. (b) X-ray pattern of the material at 600 °C with peaks of anatase marked "a" and those of the hexatitanate phase "h". (c) Area under the (1 1 0) peak of the titanate and area under the (1 0 1) peak of anatase as a function of temperature.

nate to 0.25°, and fixing the anatase (1 0 1) peak to its known 2θ position at that temperature.

The calcination of the as-synthesized potassium titanates was also investigated using differential thermal analysis (DTA)/thermogravimetric analysis (TGA) (Figure 6). A mass loss of approximately 14% was observed between room temperature and 400 °C, which was assigned to the departure of adsorbed water or surface hydroxy ions. There is a perturbation of the DTA trace at about 550 °C, evidently due to the formation of anatase reaching its maximum rate at that temperature. Heating beyond 600 °C caused a further 3.2% loss in mass, the rate of which peaked at 818 °C.

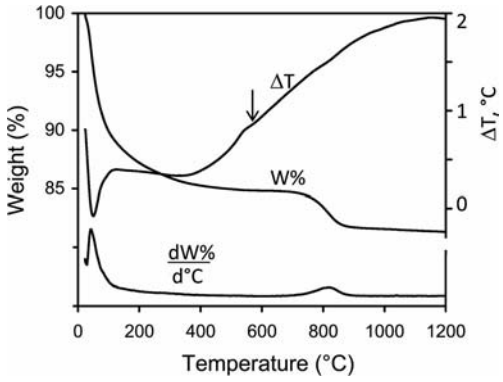

Figure 6. DTA/TGA of as-synthesized potassium titanate. The arrow on the curve for ΔT indicates the peak rate of anatase formation.

The powder diffraction patterns of the sodium-rich fibers after calcination are shown in Figure 7. Surprisingly, no significant change to the sodium titanate had occurred by 617 °C and it was therefore heated to 800 °C. Recrystallization of the $M_2Ti_6O_{13}$ phase occurred above 620 °C (Figure 7, (a) as evidenced by the sharpening of the individual peaks Figure 7, b). There was a steep increase in the height of the diffraction peaks but no corresponding change in their area (Figure 7, c) as expected for a process that does not create a new phase.

The hydrogen-rich titanate material was converted to anatase, but at a higher temperature than the potassium-rich starting fibers, with scarcely any anatase evident by 600 °C. However, above 600 °C formation was rapid, and the biggest anatase (1 0 1) peak was obtained at 702 °C, Figure 8. Curiously, above 700 °C, the peak area of the anatase produced from the hydrogen-rich fibers started to decrease again. This decrease was due to a time-dependent process, which was confirmed by holding the sample at 812 °C for a protracted time (Figure S1, Supporting Information).

The reduction in peak area may have been due to the reported conversion of anatase to aperiodic titania as the first step in the reconstructive transformation of anatase to rutile[33] or due to the possibility that some of the ostensible peak area for the anatase overlapped that of a diminishing quantity of residual $M_2Ti_6O_{13}$.

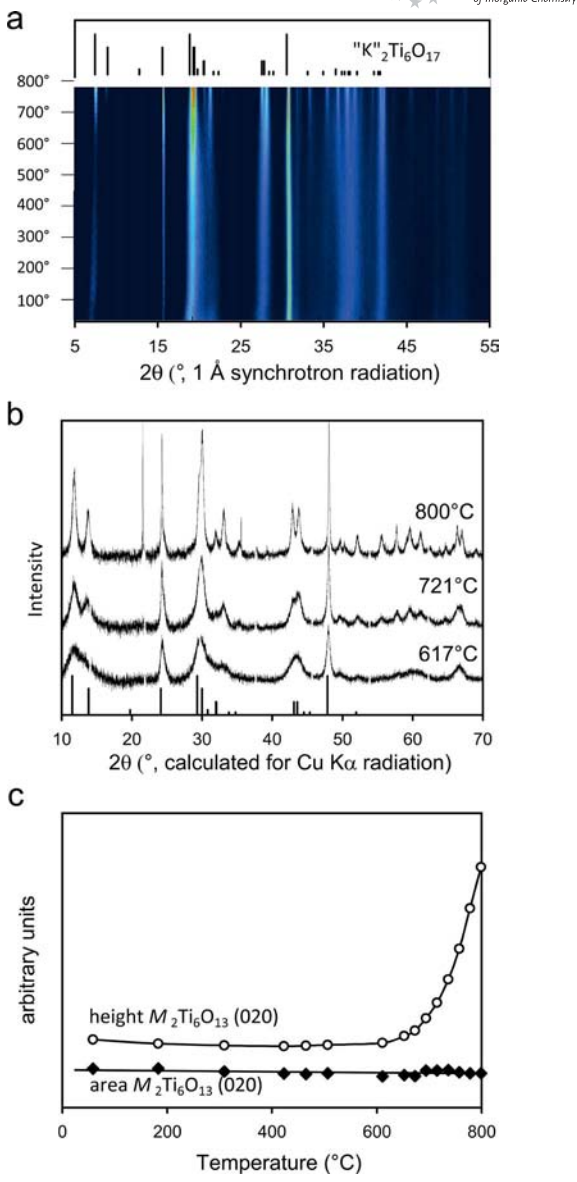

Figure 7. (a) In situ X-ray diffraction patterns of products formed by calcining the sodium-rich sample. The JCPDS pattern for $K_2Ti_6O_{13}$ is shown as a stick plot and it is evident that the sodium-rich sample has the same structure. (b) Individual X-ray patterns at selected temperatures, which show sharpening of the peaks as the structure recrystallized. The stick plot is for $K_2Ti_6O_{13}$. (c) Height and area of the (0 2 0) peak of $M_2Ti_6O_{13}$ at temperatures above 600 °C. Note that the area of the peak does not change significantly, which indicates that the volume fraction of the $M_2Ti_6O_{13}$ phase does not change.

The ammonium-rich titanate was also converted to anatase, but even more slowly than the hydrogen-rich material (Figure 9). It is evident, however, that the process was far from complete at 760 °C (Figure 9, a) with the anatase formed at that temperature characterized by broad peaks. It is possible that the presence of NH_4^+ caused significant amorphization of the titanate fiber structure. The formation of anatase in the potassium-, hydrogen-, and supposedly ammonium-rich fibers is compared in Figure 9 (b).

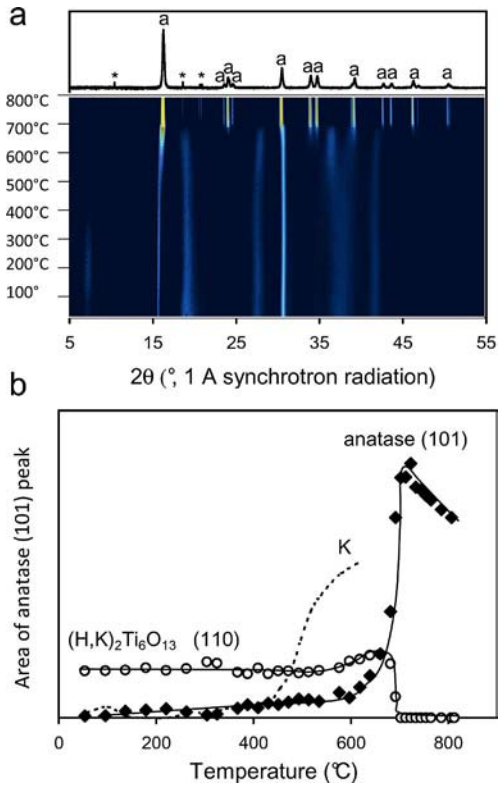

Figure 8. (a) X-ray diffraction map showing conversion of the hydrogen-rich titanate sample to anatase. The peaks corresponding to anatase are marked the letter a. An unknown phase (peaks marked asterisks *) was also formed at elevated temperature. This unknown phase is not rutile. (b) Integrated areas of the $M_2Ti_6O_{13}$ (1 1 0) and anatase (1 0 1) peaks for the hydrogen-rich titanate. The trend line for the original as-synthesized potassium-rich titanate is shown as a dashed line. It is clear that the conversion of hydrogen-rich material began at a higher temperature than for the original potassium-rich material, but was very rapid once initiated.

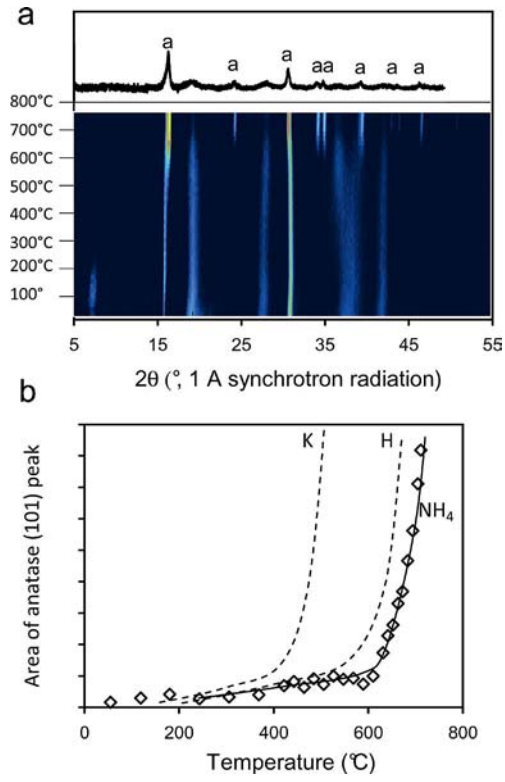

Figure 9. (a) X-ray diffraction map showing conversion of the ammonium-rich sample to anatase. The reaction is quite retarded and incomplete at 760 °C and (b) relative to the other samples examined.

Photocatalytic Efficacy

Data from photocatalysis experiments using the as-prepared potassium-rich fibers and the potassium-rich product that had been calcined for 4 h at 700 °C are shown in Figure 10. Both forms are photocatalysts for the oxidation of methylene blue and rhodamine 6G, although the calcined material is significantly more active. Importantly, we found that the as-synthesized fibers could be collected on a filter paper to produce a permeable mat, which was utilized as an effective photocatalytic substrate (Figure 10, c).

Discussion

This work has highlighted that the thermal stability of titanate fibers prepared in KOH is very sensitive to their chemical composition, with very different results obtained upon the calcination of the four samples prepared here, despite the similarity of their starting structures. We have shown that ion-exchange of the alkali metal with hydrogen or ammonium did not destroy the titanate structure, which is similar to that in some reports[21] but in contrast to others who found that anatase or TiO_2-B was formed.[2,3,15,18,34] On the other hand, sonication in water broke up the fibers and converted them to a nanocrystalline form of TiO_2. It is clear that conditions should be carefully controlled if the fibrous titanate morphology and desired mix of intercalated cations are to be retained.

The stoichiometry of the intercalated counterion in this type of titanate can be variable, with K^+, H^+, Na^+, and NH_4^+ capable of substituting partially or fully for one another. This is similar to the situation for titanate fibers produced by digestion in NaOH.[2,4,21,23] Similarly, the calcination of the potassium-, sodium-, and hydrogen-rich materials synthesized here followed similar trends to those reported for fibers prepared using NaOH. For example, in both cases the hydrogen-rich material produced by ion exchange of the original alkali metal decomposes to anatase[2,3] with a rod-like shape,[35][23] whereas for the NaOH fibers, material that was high in alkali metal content did not form anatase and instead recrystallized as a mixed alkali metal hexatitanate.[4,5,21,23,36] On the other hand, the ammonium-rich titanate produced here was relatively resistant to calcination unlike that reported by Rhee et al.,[31] which readily decomposed to a mixture of anatase and $TiO_{2-x}N_x$ on heating above 290 °C.

The X-ray diffraction patterns of the fibers produced are consistent with a compound with the stoichiometry

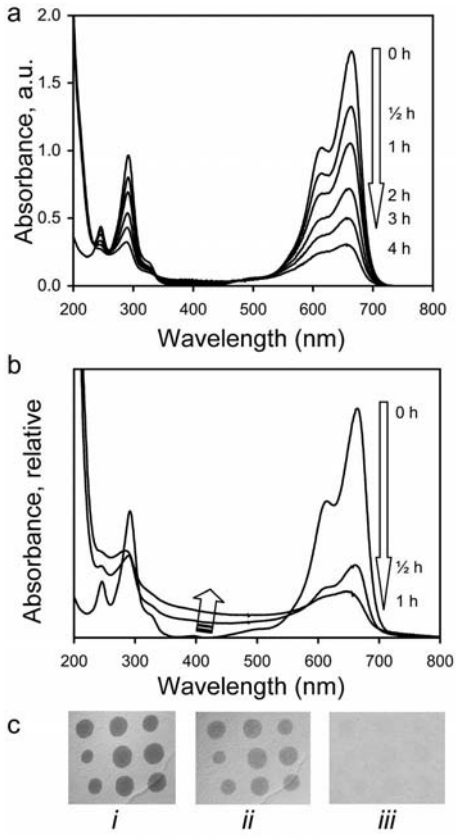

Figure 10. Photocatalytic action of (a) as-synthesized potassium-rich nanofibers and (b) nanofibers calcined at 700 °C on methylene blue. In (b) the absorbances were affected by an increasing amount of turbidity (arrow at 400 nm) as the reaction proceeded, and the results shown here have been vertically offset to give a zero absorbance at 820 nm for comparison. (c) Effect of sunlight on rhodamine 6G stains applied to a mat of as-synthesized potassium-rich fibers (*i*: no exposure, *ii*: 30 min, and *iii*: 3 h).

$M_2Ti_6O_{13}$, where M can be a variable mix of K^+, Na^+, H^+ or (evidently) NH_4^+. This is quite unlike the case for fibers produced in NaOH, where it seems that a trititanate of the generic form $Na_{2-x}H_xTi_3O_7{\cdot}nH_2O$ is the most likely product.[4] However, as mentioned earlier, not all reports of the use of KOH have led to $M_2Ti_6O_{13}$, so there remain some puzzling inconsistencies (Table 1). These inconsistencies could be due to factors such as the strength of the acid used to wash the fibers and the nature of the starting seed material. These factors also affect the extent to which K^+ is extracted from the fibers during washing, possibly explaining why some groups obtained potassium titanate fibers and others hydrogen titanate fibers (Table 1). Further work is needed to fully resolve these issues.

The difficulty in making an unambiguous phase assignment of the X-ray diffraction pattern appears to be a typical problem for titanate fibers produced by aqueous processing. Even in the case when the more common NaOH process is used to make fibers, there is still ongoing debate on the identity of the resulting phases.[4,18,19] Furthermore, a range of stoichiometries may be reported; for example, compounds such as $H_2Ti_3O_7$ or, if not fully ion exchanged, $Na_{2-x}H_xTi_3O_7$. nH_2O, $Na_2Ti_6O_{13}$, $Na_2Ti_3O_7$, $H_2Ti_4O_9{\cdot}H_2O$, and $H_2Ti_2O_4(OH)_2$ are mentioned for the NaOH process.[4,7,21] Some authors prefer to designate the product as being of somewhat variable stoichiometry, e.g. $Na_xTiO_{2+\delta}$,[20] or $H_2Ti_xO_{2x+1}{\cdot}nH_2O$,[19] whereas others find that the product resulting from the NaOH process is all or partially TiO_2 in the anatase, rutile, brookite or TiO_2-B forms,[2,15,17] i.e. not a titanate at all. Note that TiO_2-B can also exist in a layered, nanotube form,[6] so a nanofiber morphology is not conclusive evidence of titanate formation. As the Na^+ in the material produced in NaOH solution is readily interchanged with other ions, including K^+, it might reasonably be expected that the titanates made in NaOH and KOH processes would be isomorphous. This is evidently not the case and the reason is currently unknown. However, it is interesting to note that there is a report in which the sodium ions in $Na_2Ti_3O_7$ (produced by the reaction between TiO_2 and Na_2CO_3 at 1000 °C) were exchanged for potassium ions to produce fibers identified as $K_2Ti_6O_{13}$.[37] Due to the difference in crystal structure and stoichiometry between the tri- and hexatitanate, considerable solid-state rearrangement of TiO_6 octohedra must have taken place during that reaction.

Although there are certainly some titanates that are well-established as photocatalysts, e.g. $SrTiO_3$,[38] the situation for the nanofibers or nanotubes produced by hydrothermal treatment is not as clear.[23] Indeed, the question of photocatalytic efficacy is apparently not even entirely settled for the different TiO_2 structures themselves.[39] At the very least, however, charge separation (an exciton) must form in the material as a result of irradiation with light if any photocatalysis is to take place. If it does not form, then the energy of the incoming photon is likely to be radiated (photoluminescence) instead of being transferred to a chemical reaction. Riss et al.[23] reported that no charge separation occurs in $Na_2Ti_3O_7$, whereas it does occur in $H_2Ti_3O_7$. From this finding one could deduce that, of the two, only the latter is capable of photocatalysis. Qamar[4] cites four reports that state that the as-synthesized fibers produced by NaOH digestion are photocatalysts and four reports to the contrary but found that their own $Na_{2-x}H_xTi_3O_7{\cdot}nH_2O$ was inert. It is known, however, that the efficacy of the catalyst depends acutely on the reaction being photocatalyzed[39] and there are persistent reports of photocatalysis in uncalcined fibers under particular circumstances.[5,21,27]

We have shown that the as-synthesized potassium-rich titanate is certainly active for the oxidation of methylene blue, although not as active as the anatase that it formed by calcination. This result is broadly consistent with the verdict of Amano et al.[5] who found that the photocatalytic efficacy of what they described as $K_xH_{2-x}Ti_4O_9$ depends on the reaction being studied, and has, for example, little efficacy for oxidation of acetic acid but excellent efficacy for the generation of hydrogen from methanol. This group also reported that bulk $K_2Ti_4O_9$ and bulk $K_2Ti_6O_{13}$ were good photocatalysts. In all cases, calcination improved the efficacy.

Conclusions

Potassium-rich nanofibers have been prepared from TiO_2 powder by reaction with KOH under hydrothermal conditions. These nanofibers have the $K_2Ti_6O_{13}$ crystal structure, although EDS analysis suggested that the K was partially substituted with H to give a stoichiometry of approximately $(K_{0.5}H_{0.5})_2Ti_6O_{13}$. In the as-synthesized condition the fibers were photocatalytically active with respect to the decoloration of methylene blue and rhodamine 6G under illumination with UV light. In addition, the fibers could be collected as mats, which were also catalytic. This aspect has important implications for the preparation of porous, photocatalytic textile-like filter fabrics, which could be used in water purification applications.

The potassium content of the fibers could be reduced by ion exchange, and a hydrogen-rich fiber of approximately $(K_{0.26}H_{0.74})_2Ti_6O_{13}$ composition, a sodium-rich fiber of $(K_{0.3}Na_{0.7})_2Ti_6O_{13}$ and an ammonium-doped fiber of $(K_{0.26}Na_{0.11}X_{0.63})_2Ti_6O_{13}$, where X is assigned as NH_4^+, were produced.

Calcination of the potassium-rich fibers converted them to anatase and improved the catalytic efficacy but led to some loss of the desirable fibrous morphology. The hydrogen- and ammonium-rich fibers also converted to anatase during calcination, although not as rapidly as the potassium-rich fiber. In contrast, the sodium-rich fiber recrystallized as $M_2Ti_6O_{13}$ and did not appreciably form anatase below 800 °C.

It is clear that the structure and activity of these titanate fibers varies in a sensitive manner in response to the method of their preparation, washing, ion-exchange or calcination. This contribution provides further insight into these factors but there are still many other interesting aspects to address and clarify before these potentially useful materials can be fully exploited.

Experimental Section

General: Nanofibers were produced by a hydrothermal process. TiO_2 powder (Degussa P25, 0.3 g) was treated with an aqueous KOH solution (10 M, 30 mL) at 170 °C for 7 d in a Teflon®-lined autoclave container. The choice of a 7 d duration was motivated by some previous reports,[25,27] however, it is possible that a shorter treatment (of the order of 2 d) might also have been viable. The reaction products were washed with diluted HCl (0.1 M) and distilled water until neutralized and dried at 80 °C for 12 h. This material is designated here as potassium-rich titanate. The subsequent ion-exchange of the as-synthesized material was carried out as follows: first H^+ was exchanged for K^+ by immersion of the potassium-rich titanate (300 mg) in 2 M aqueous HCl (50 mL) at room temperature for 12 h. A portion of the hydrogen-rich titanate (100 mg) was treated with a 1 M aqueous NaOH solution (20 mL) and stirred for 24 h to give the sodium-rich titanate. A portion of this product was treated in a 5 M aqueous NH_4OH solution (20 mL) for 24 h to yield the ammonium-rich titanate.

A crude assessment of the photocatalytic activity of the materials was made by using aqueous solutions of methylene blue ($C_{16}H_{18}ClN_3S$, 8 μg/mL) and rhodamine 6G ($C_{28}H_{31}N_2O_3Cl$, 10 μg/mL) as colorimetric indicators. The reaction of methylene blue was followed using UV/Vis spectroscopy with an Agilent 8453 UV/Vis spectrophotometer irradiated with 254 nm UV light. The rhodamine 6G sample was made by spotting the dye solution on to a titanate mat and exposing it to natural sunlight. Control tests confirmed that, in the absence of photocatalyst, neither dye bleached visibly under the test conditions imposed.

SEM imaging and EDS analyses were performed with a Zeiss Supra SEM, which used an Oxford Microanalysis System beam voltage of 10 keV, 30 μm aperture, working distance of 6 mm, and Cu-K_α and L lines. A 100 s count time gave ca. 1000 counts, and an average was obtained using at least six measurements. The processing was standardless. The method can accurately determine the ratio of the heavier elements to one another but cannot determine the hydrogen content. However, once the basic $M_2Ti_6O_{13}$ stoichiometry had been determined by XRD, SEM EDS could be used to estimate the degree to which M had been substituted with other ions.

TEM experiments used a small amount of powder (ca. 1×1 mm pile) placed in a clean plastic sample tube. Water (approx. 3 mL) and ethanol (approx. 500 μL) were added so that the total solvent contained < 20 vol.-% ethanol. The samples were sonicated in an unheated water bath for 30 min. About 0.2 mL of the suspension was pipetted onto a holey carbon grid, which was left to dry for 15 min under an incandescent lamp.

In situ synchrotron XRD experiments were performed in 0.3 mm diameter SiO_2 (quartz) capillaries using the Powder Diffraction Beamline of the Australian Synchrotron. A Mythen II microstrip detector was employed to acquire the diffraction data and the capillaries (containing powders) were continuously rotated during data collection to improve the particle statistics. Scans were normalized against the integrated ion chamber count. The background was subtracted using the blank run of an empty quartz capillary. A LaB_6 660a standard reference material was used to calibrate the wavelength (0.998304 ± 0.000004 Å).

Thermal analysis was carried out with a SDT 2960 machine (TA Instruments Inc., USA) with a heating rate of 5 °C min^{-1} in a N_2 stream.

Supporting Information (see footnote on the first page of this article): Figure showing time-dependent decrease in area under anatase (1 0 1) peak for hydrogen-rich starting material held at 812 °C.

Acknowledgments

The authors thank Dr R. Wuhrer of the Microstructural Analysis Unit of the University of Technology Sydney for his support. Part of this research was undertaken on the Powder Diffraction Beamline at the Australian Synchrotron, Victoria, Australia.

[1] D. V. Bavykin, J. M. Friedrich, F. C. Walsh, *Adv. Mater.* **2006**, *18*, 2807.
[2] J. S. Church, A. L. Woodhead, K. Fincher, *J. Colloid Interface Sci.* **2010**, *346*, 43.
[3] X. Zhang, A. J. Dua, P. Lee, D. D. Sun, J. O. Leckie, *J. Membr. Sci.* **2008**, *313*, 44.
[4] M. Qamar, C. R. Yoon, H. J. Oh, N. H. Lee, K. Park, D. H. Kim, K. S. Lee, W. J. Lee, S. J. Kim, *Catal. Today* **2008**, *131*, 3.
[5] F. Amano, T. Yasumoto, T. Shibayama, S. Uchida, B. Ohtani, *Appl. Catal. B* **2009**, *89*, 583.
[6] G. Armstrong, A. R. Armstrong, J. Canales, P. G. Bruce, *Chem. Commun.* **2005**, 2454.

[7] H. Y. Niu, J. M. Wang, Y. L. Shi, Y. Q. Cai, F. S. Wei, *Microporous Mesoporous Mater.* **2009**, *122*, 28.
[8] S.-S. Liu, C.-K. Lee, H.-C. Chen, C.-C. Wang, L.-C. Juang, *Chem. Eng. J.* **2009**, *147*, 188.
[9] D. J. Yang, Z. F. Zheng, H. Y. Zhu, H. W. Liu, X. P. Gao, *Adv. Mater.* **2008**, *20*, 2777.
[10] J.-M. Herrmann, *Catal. Today* **1999**, *53*, 115.
[11] A. Fujishima, K. Honda, *Nature* **1972**, *238*, 37.
[12] W. Dong, A. Cogbill, T. Zhang, S. K. Ghosh, Z. R. Tian, *J. Phys. Chem. B* **2006**, *110*, 16819.
[13] S.-U. Geissen, W. Xi, A. Weidemeyer, A. Vogelpohl, L. Bousselmi, A. Ghrabi, A. Ennabli, *Wat. Sci. Technol.* **2001**, *44*, 245.
[14] D. F. Ollis, *Ann. N. Y. Acad. Sci.* **2003**, *984*, 65.
[15] T. P. Feist, P. K. Davies, *J. Solid State Chem.* **1992**, *101*, 275.
[16] T. Kasuga, M. Hiramatsu, A. Hoson, T. Sekino, K. Niihara, *Langmuir* **1998**, *14*, 3160.
[17] W. A. Daoud, G. K. H. Pang, *J. Phys. Chem. B* **2006**, *110*, 25746.
[18] Y. Zhou, C. Liu, M. He, X. Lu, X. Feng, Z. Yang, *J. Mater. Sci.* **2008**, *43*, 155.
[19] D. V. Bavykin, F. C. Walsh, *J. Phys. Chem. C* **2007**, *111*, 14644.
[20] A. Magrez, L. Horváth, R. Smajda, V. Salicio, N. Pasquier, L. Forró, B. Schwaller, *ACS Nano* **2009**, *3*, 2274.
[21] J. S. Church, K. Fincher, X. Wang, *Aust. J. Chem.* **2010**, *63*, 293.
[22] G. H. Du, Q. Chen, R. C. Che, Z. Y. Yuan, L.-M. Peng, *Appl. Phys. Lett.* **2001**, *79*, 3702.
[23] A. Riss, M. J. Elser, J. Bernardi, O. Diwald, *J. Am. Chem. Soc.* **2009**, *131*, 6198.
[24] A. Riss, T. Berger, H. Grothe, J. Bernardi, O. Diwald, E. Knözinger, *Nano Lett.* **2007**, *7*, 433.
[25] T. J. Boyle, T. N. Lambert, H. D. Pratt III, P. Lu, J. J. M. Griego, N. Bush, C. A. Chavez, M. Welk, *J. Mater. Sci.* **2010**, *45*, 1744.
[26] X. Meng, D. Wang, J. Liu, B. Lin, Z. Fu, *Solid State Commun.* **2006**, *137*, 146.
[27] A. Nakahira, W. Kato, M. Tamai, T. Sishiki, K. Nishio, H. Aritani, *J. Mater. Sci.* **2004**, *39*, 4239.
[28] Z.-Y. Yuan, X.-B. Zhang, B.-L. Su, *Appl. Phys. A* **2004**, *78*, 1063.
[29] G. H. Du, Q. Chen, P. D. Han, Y. Yu, L.-M. Peng, *Phys. Rev. B* **2003**, *67*, 035323.
[30] J. Vasquez, H. Lozano, V. Lavayen, M. Lira-Cantú, P. Gómez-Romero, M. A. S. Ana, E. Benavente, G. Gonzalez, *J. Nanosci. Nanotechnol.* **2009**, *9*, 1103.
[31] C. H. Rhee, J. S. Lee, S. H. Chung, *J. Mater. Res.* **2005**, *20*, 3011.
[32] L. M. Shen, N. Z. Bao, Y. Q. Zheng, A. Gupta, T. C. An, K. Yanagisawa, *J. Phys. Chem. C* **2008**, *112*, 8809.
[33] S. H. Lim, C. Ritter, Y. Ping, M. Schreyer, T. J. White, *J. Appl. Crystallogr.* **2009**, *42*, 917.
[34] H. Y. Zhu, Y. Lan, X. P. Gao, S. P. Ringer, Z. F. Zheng, D. Y. Song, J. C. Zhao, *J. Am. Chem. Soc.* **2005**, *127*, 6730.
[35] M.-C. Wu, A. Sápi, A. Avila, M. Szabó, J. Hiltunen, M. Huuhtanen, G. Tóth, Á. Kukovecz, Z. Kónya, R. Keiski, W.-F. Su, H. Jantunen, K. Kordás, *Nano Res.* **2011**, *4*, 360.
[36] E. Morgado, M. A. S. d. Abreu, G. T. Moure, B. A. Marinkovic, P. M. Jardim, A. S. Araujo, *Mater. Res. Bull.* **2007**, *42*, 1748.
[37] B. L. Wang, Q. Chen, R. H. Wang, L.-M. Peng, *Chem. Phys. Lett.* **2003**, *376*, 726.
[38] F. E. Osterloh, *Chem. Mater.* **2008**, *20*, 35.
[39] J. Ryu, W. Choi, *Environ. Sci. Technol.* **2008**, *42*, 294.

Received: June 27, 2011
Published Online: October 21, 2011

